

# Supporting Information

## Supercritical Synthesis of Magnetite-Reduced Graphene Oxide Hybrid with Enhanced Adsorption Properties toward Cobalt & Strontium Ions

Ahmad Tayyebi\*, Mohammad Outokesh\*

Department of Energy Engineering, Sharif University of Technology, Azadi Ave. P.O. Box:  
113658639, Tehran, Iran.

\*Corresponding author's email address: [Outokesh@sharif.edu](mailto:Outokesh@sharif.edu), [atayebi162@gmail.com](mailto:atayebi162@gmail.com)

**RSC Advances**

Supplemental Information, 19 Pages with 14 Figures and 2 Tables

## List of Supplemental Figures

**Figure S1:** schematic illustration of M-RGO synthesis procedure.

**Figure S2:** (a) XRD patterns of prepared materials, and (b) Raman Spectra of synthesized materials (Graphite, GO, RGO, M-RGO)

**Figure S3:** (a) Low resolution TEM image of M-RGO synthesized using supercritical methanol, and (b) corresponding size distribution of magnetite NPs with an average diameter of 15 nm.

**Figure S4:** EDX analysis of GO, RGO, and M-RGO.

**Figure S5:** DLS size distribution of  $\text{Fe}_3\text{O}_4$  NPs nanoparticles in water.

**Figure S6:** High resolution peak Fe2p core level peak.

**Figure S7:** FWHM of High resolution of O1s core level peak.

**Figure S8:** 3-Dimensional schematic illustration of methanol interaction with  $\text{Fe}_3\text{O}_4$  NPs surface.

**Figure S9:** Adsorption behavior of  $\text{Fe}_3\text{O}_4$  NPs synthesized by two different method (Ultrasound assisted chemical precipitation and supercritical methanol) for (a)  $\text{Co}^{2+}$ , and (b)  $\text{Sr}^{2+}$  ions from aqueous solution at pH 6.5 and  $T=298$  K.

**Figure S10:** Transmission electron microscopy (TEM) images of (a)  $\text{Fe}_3\text{O}_4$  NPs bulk, and (b)  $\text{Fe}_3\text{O}_4$  NPs on the surface of graphene sheet.

**Figure S11:** Linear fitting of  $\ln K_d$  vs.  $C_e$  at pH=6.5 for (a)  $\text{Co}^{2+}$  ions; and (b)  $\text{Sr}^{2+}$  ions in aqueous solutions

**Figure S12:** Vant't Hoff plot of  $\ln K^0$  versus  $1/T$  for (a)  $\text{Co}^{2+}$ , and (b)  $\text{Sr}^{2+}$  ions.

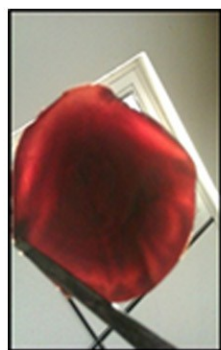
**Figure S13:** Comparison between the uptake rates in a normalized coordination (X).

**Figure S14:** Desorption of  $\text{Co}^{2+}$  ions from M-RGO using different concentration of hydrochloridric acid (HCl).

### **List of Supplemental Tables**

**Table S1:** Constants of linear fit of  $\ln K_d$  Vs.  $C_e$  ( $\ln K_d = A + BC_e$ ) for  $\text{Co}^{2+}$  removal onto M-RGO.

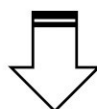
**Table S2:** Constants of linear fit of  $\ln K_d$  Vs.  $C_e$  ( $\ln K_d = A + BC_e$ ) for  $\text{Sr}^{2+}$  removal onto M-RGO.



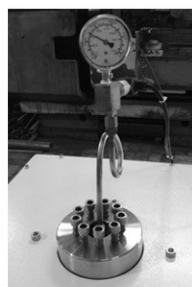
**GO Paper**



**GO Solution**



**Supercritical  
Reactor**



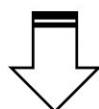
**Pressure  
Gage**



**Thermocouples &  
Coil**



**Pressure & Temperature  
Monitor**



**M-RGO Magnetite Separation**

**Figure S1:** schematic illustration of M-RGO synthesis procedure.

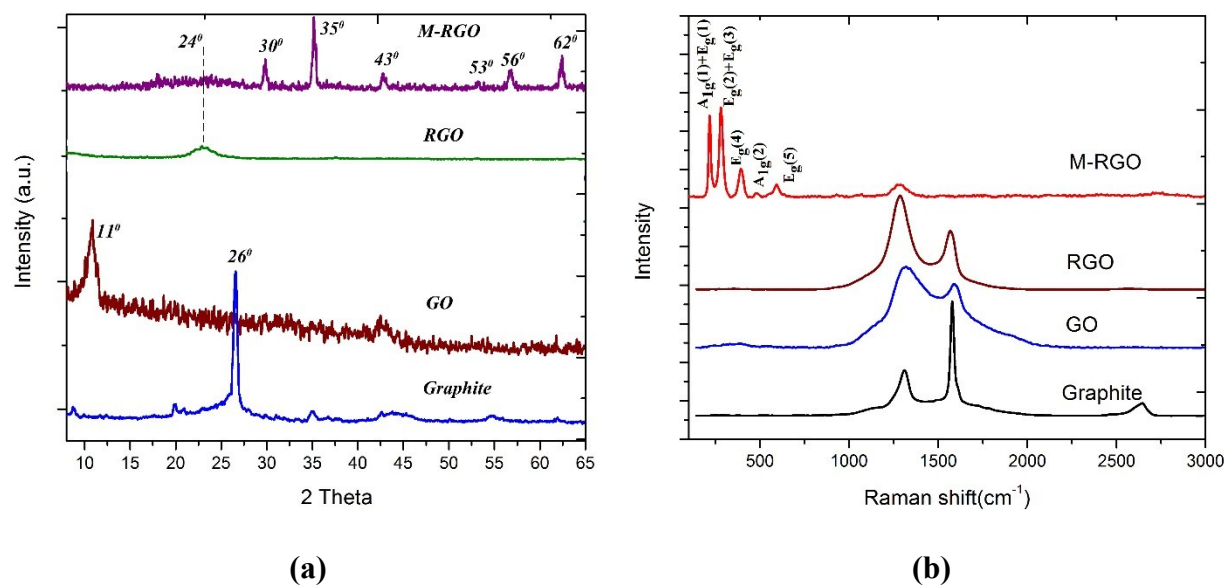
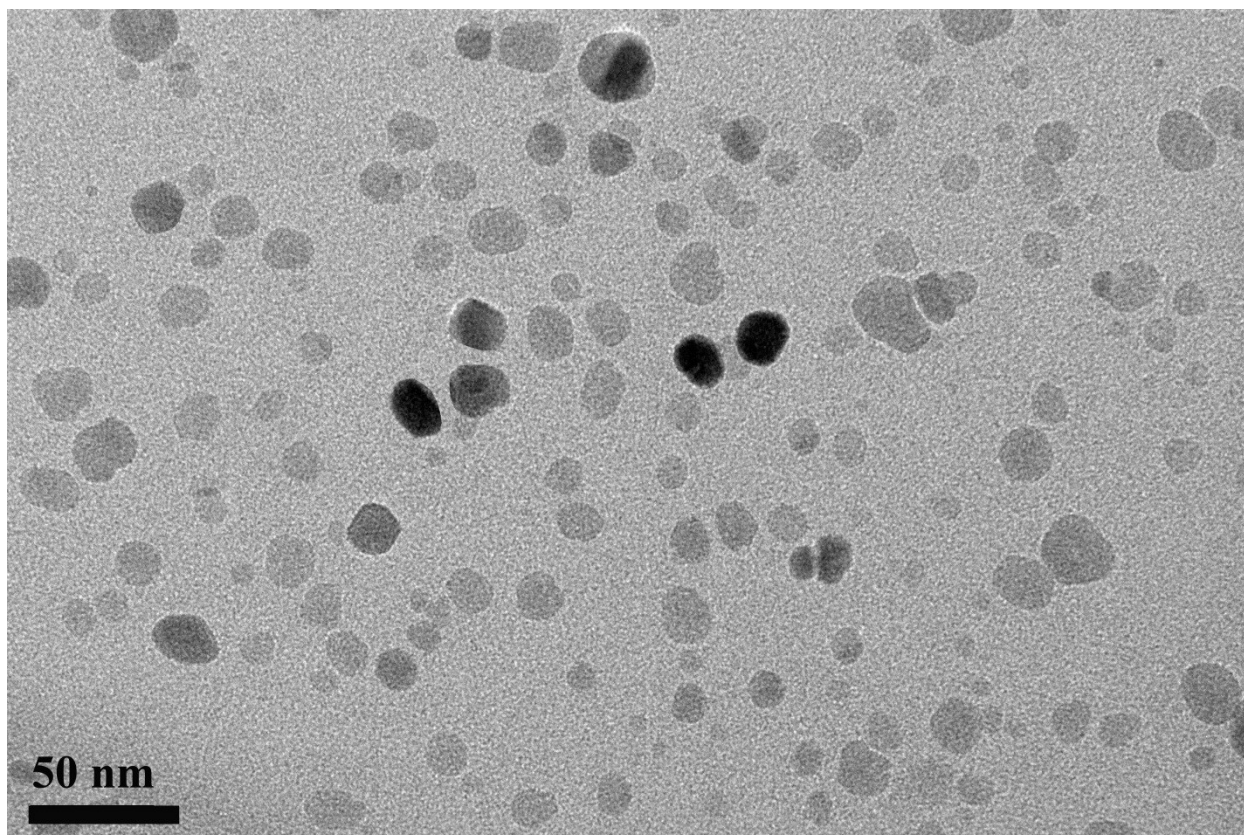
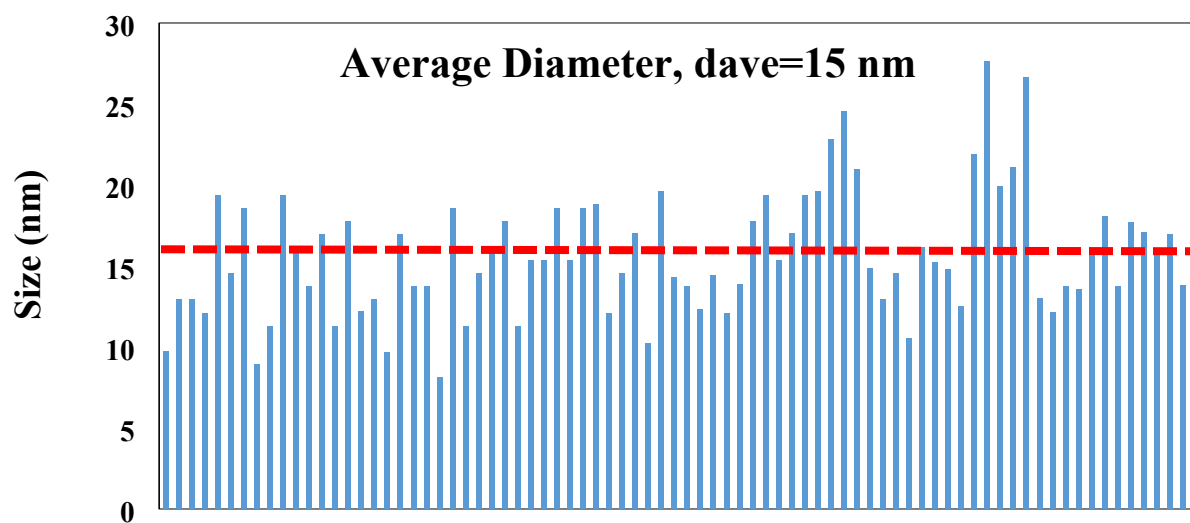


**Figure S2:** (a) XRD patterns of prepared materials, and (b) Raman Spectra of synthesized materials (Graphite, GO, RGO, M-RGO)

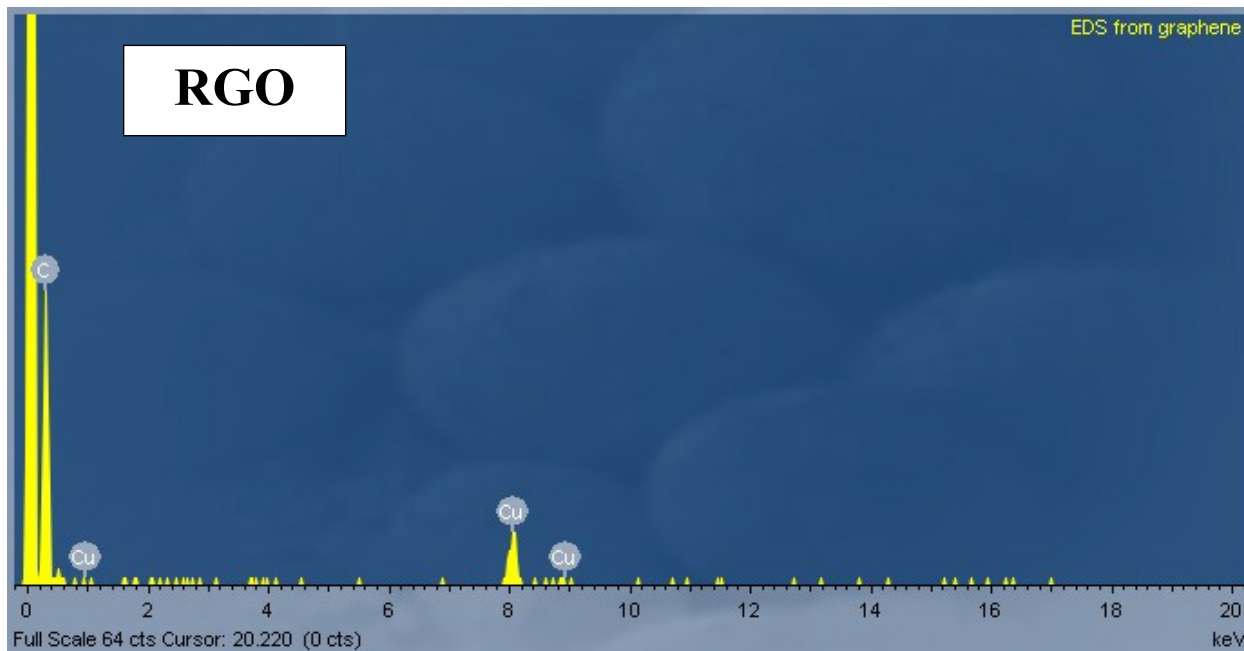
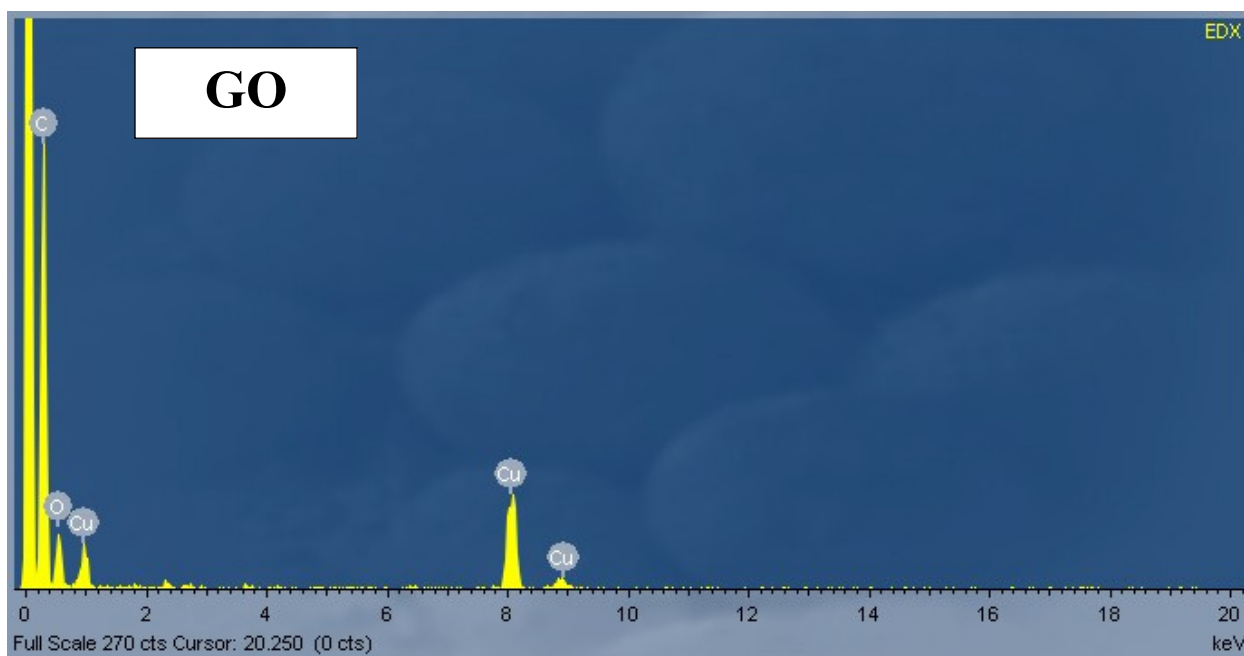


(a)



(b)

**Figure S3:** (a) Low resolution TEM image of M-RGO synthesized using supercritical methanol, and (b) corresponding size distribution of magnetite NPs with an average diameter of 15 nm.



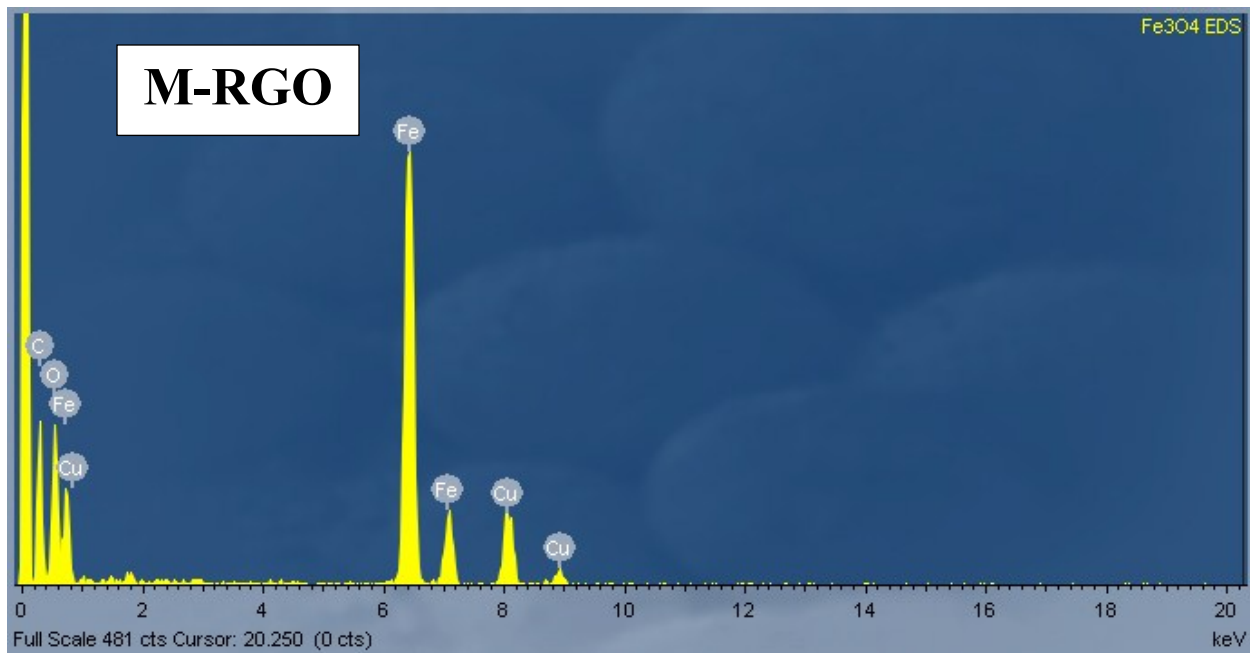


**Figure S4:** EDX analysis of GO, RGO, and M-RGO.



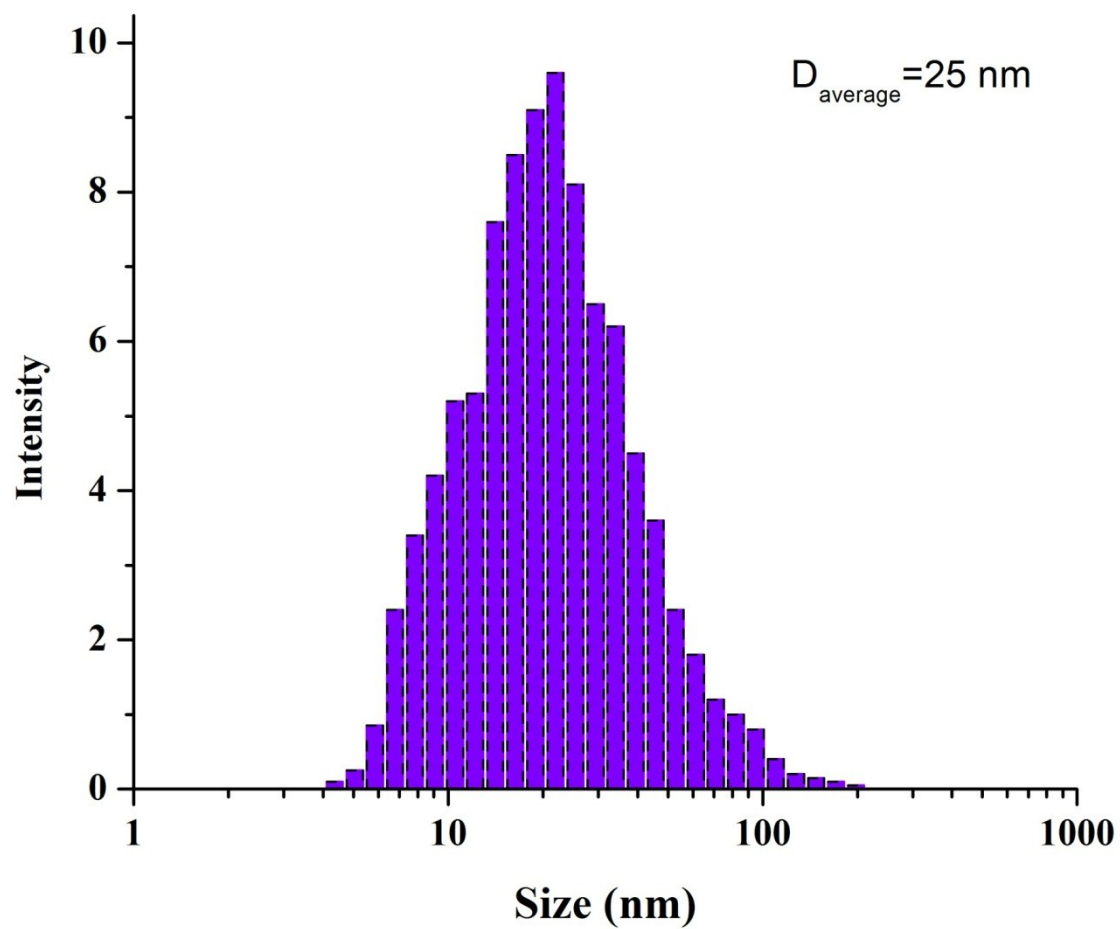


**Figure S5:** DLS size distribution of Fe<sub>3</sub>O<sub>4</sub> NPs nanoparticles in water.

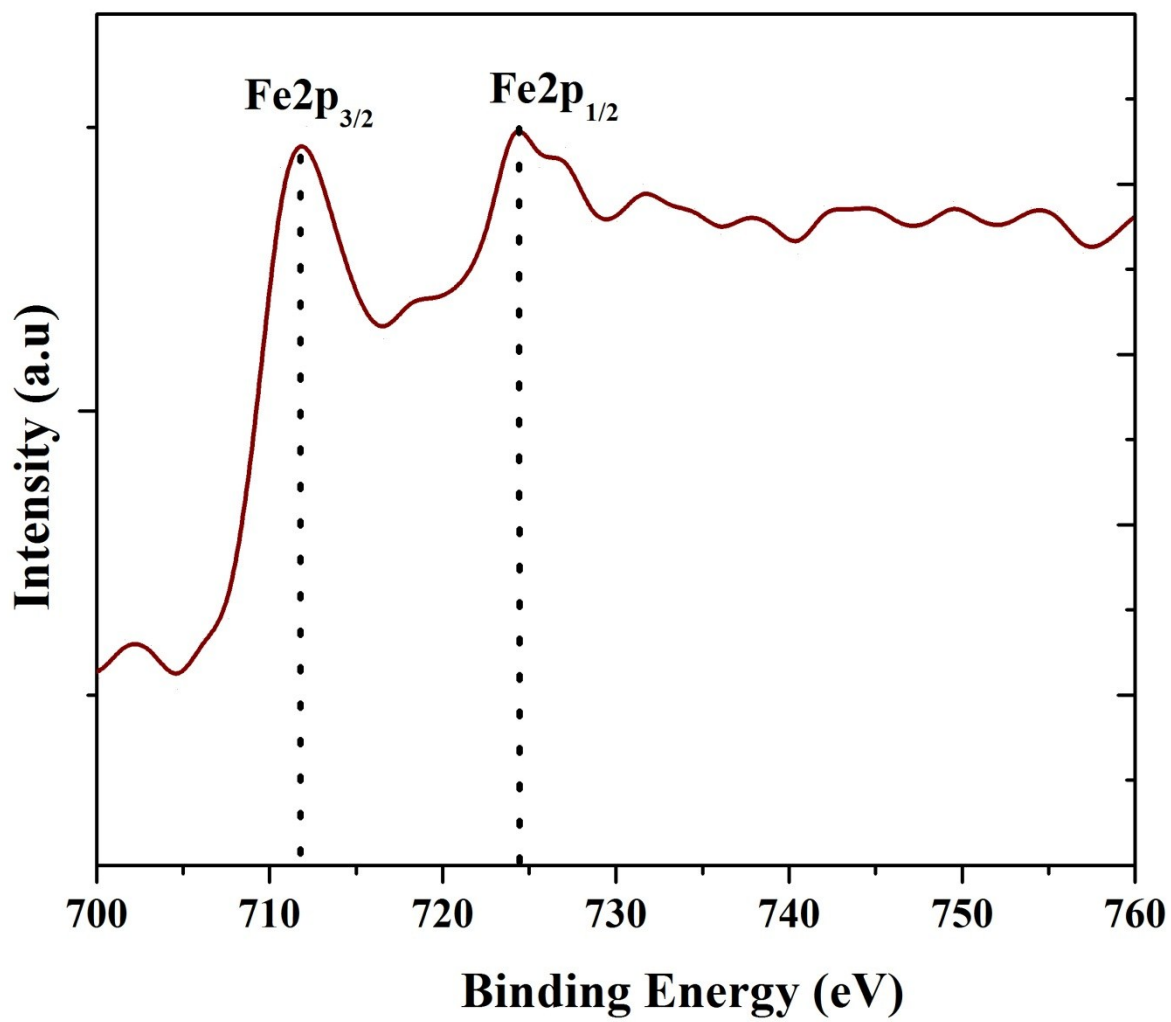


**Figure S6:** High resolution peak Fe2p core level peak.

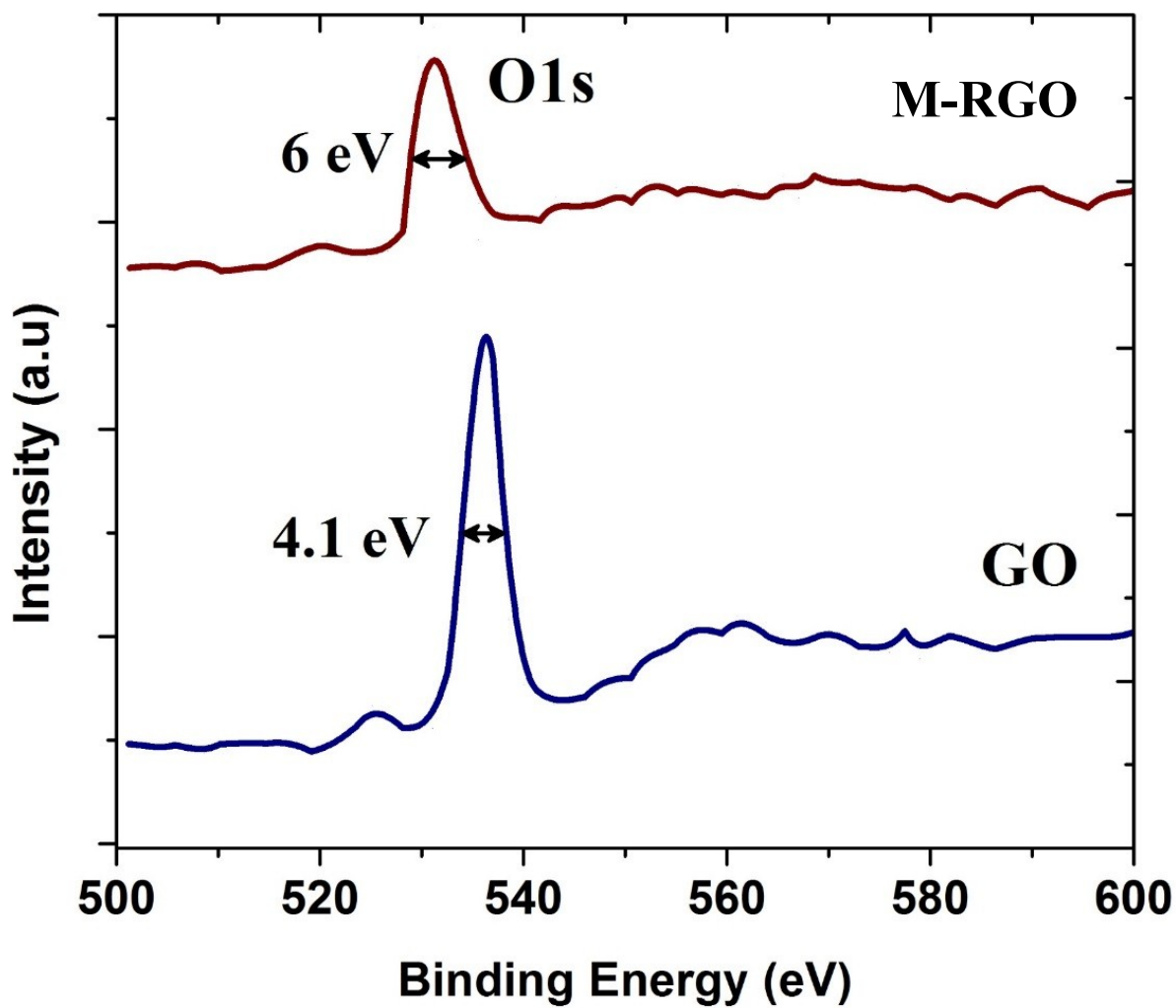
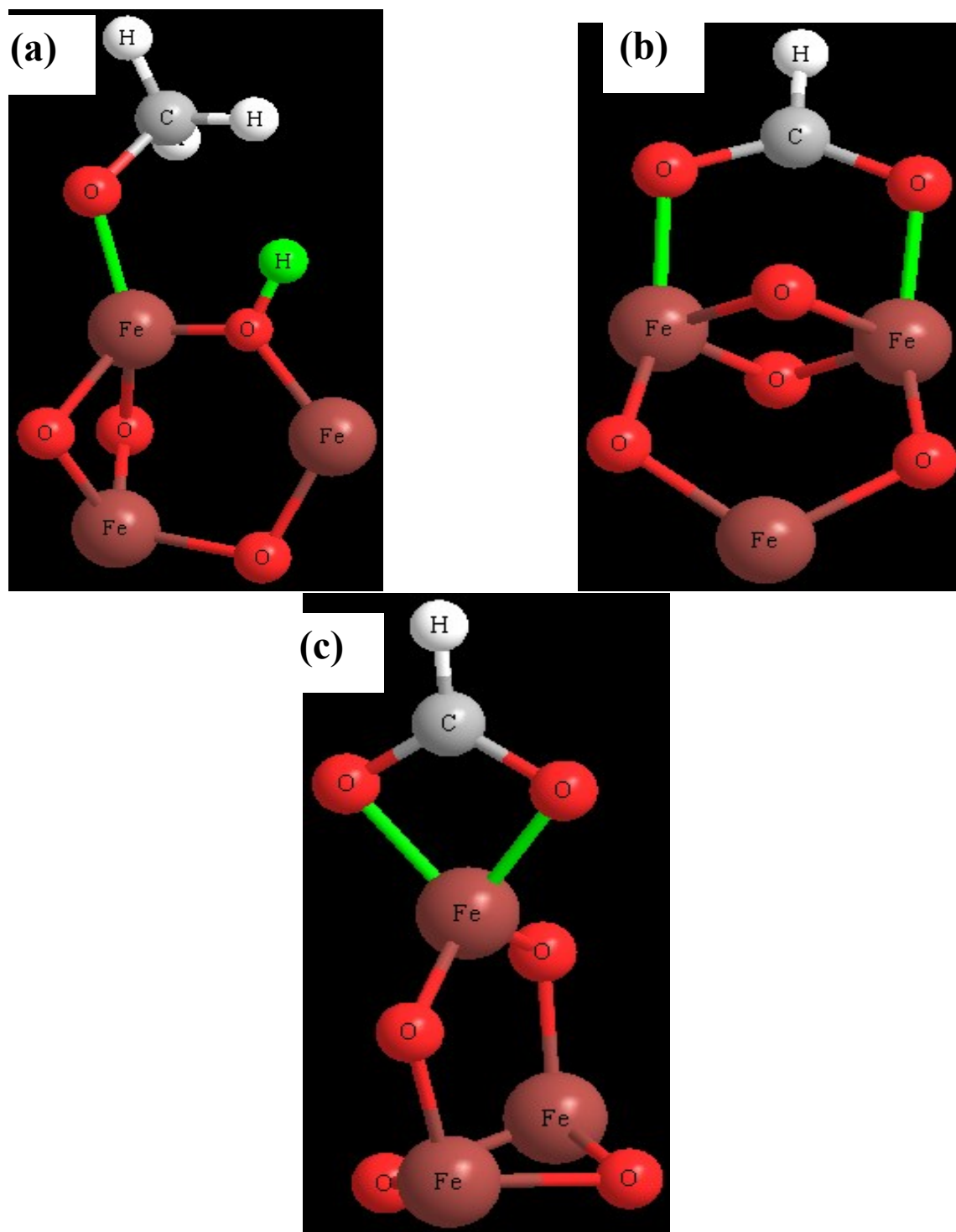
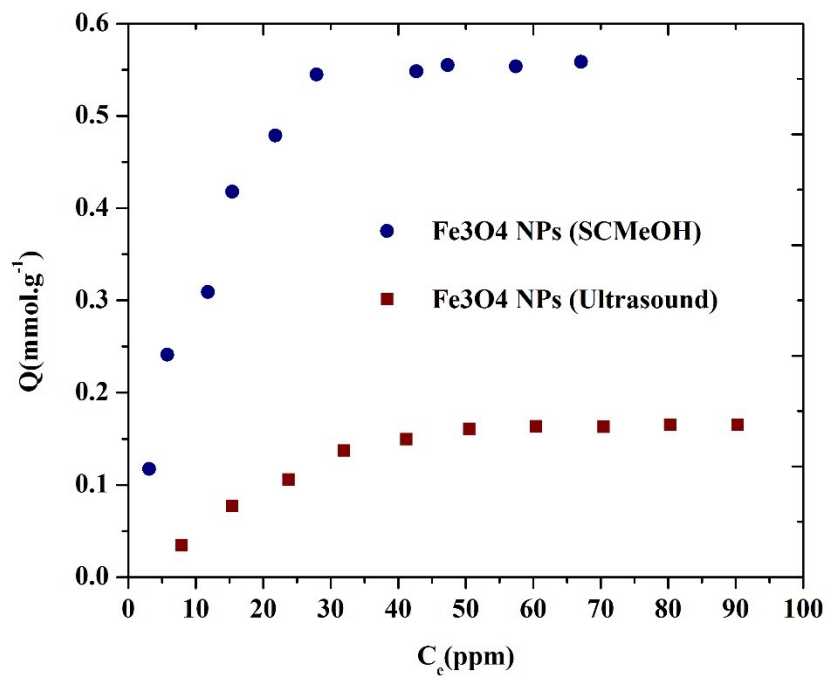


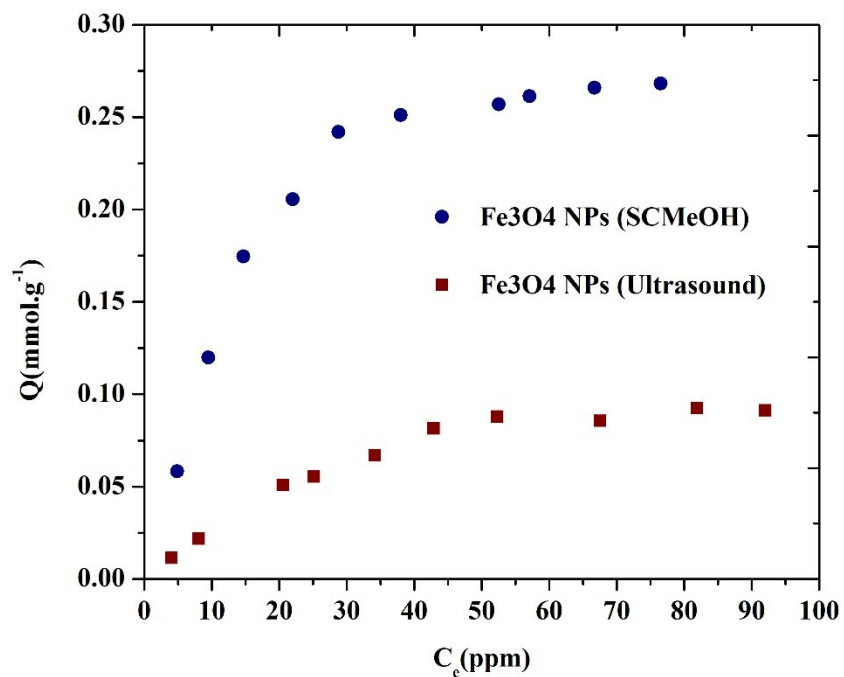
Figure S7: FWHM of High resolution of O1s core level peak.



**Figure S8:** 3-Dimensional schematic illustration of methanol interaction with Fe<sub>3</sub>O<sub>4</sub> NPs surface.



(a)



(b)

**Figure S9:** Adsorption behavior of Fe<sub>3</sub>O<sub>4</sub> NPs synthesized by two different method (Ultrasound assisted chemical precipitation and supercritical methanol) for (a) Co<sup>2+</sup>, and (b) Sr<sup>2+</sup> ions from aqueous solution at pH 6.5 and T=298 K.

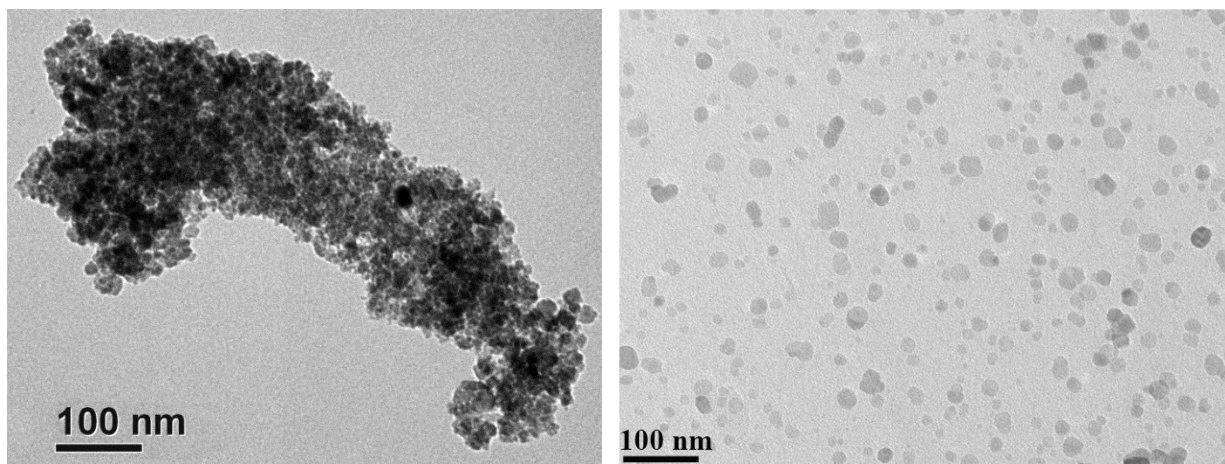
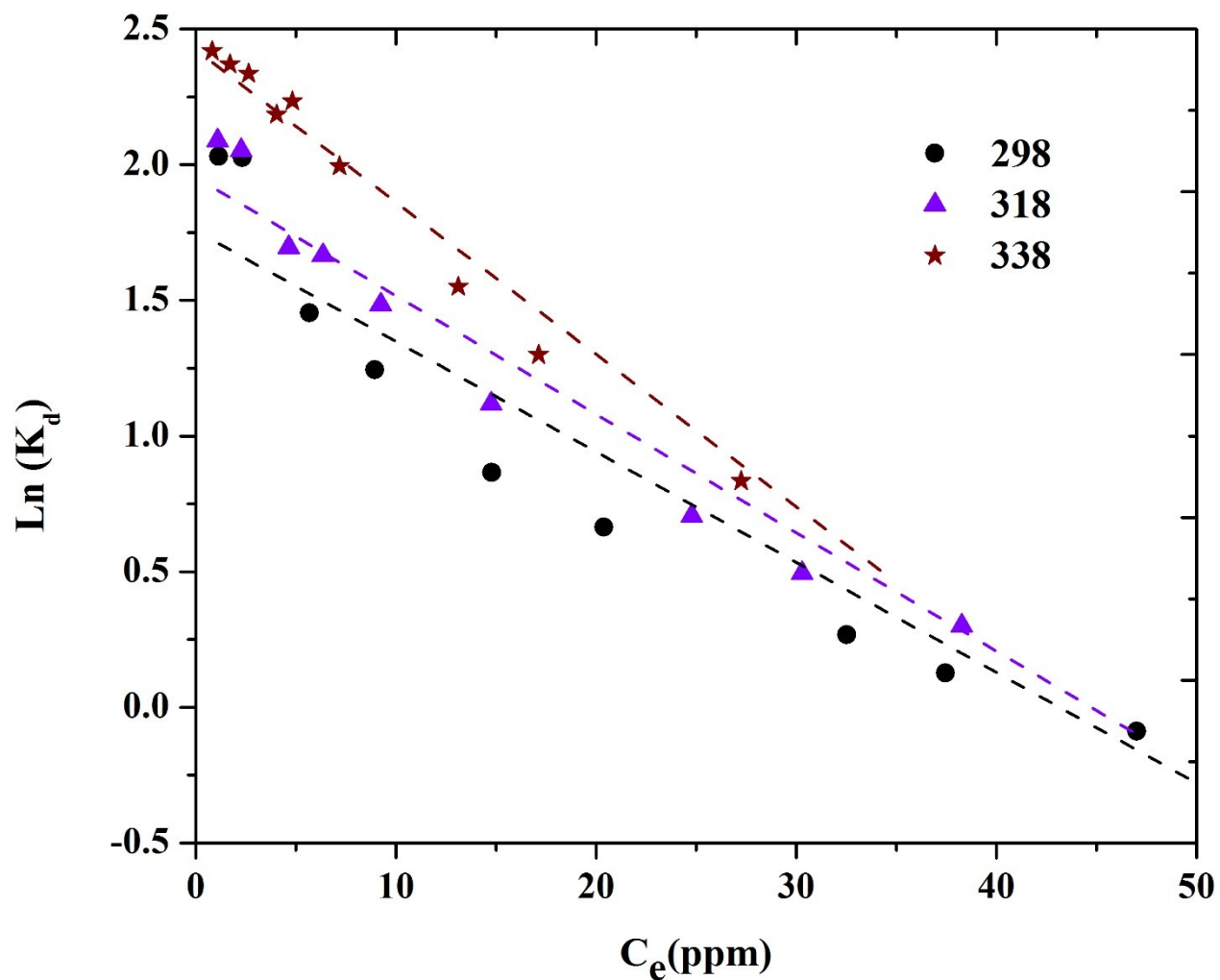


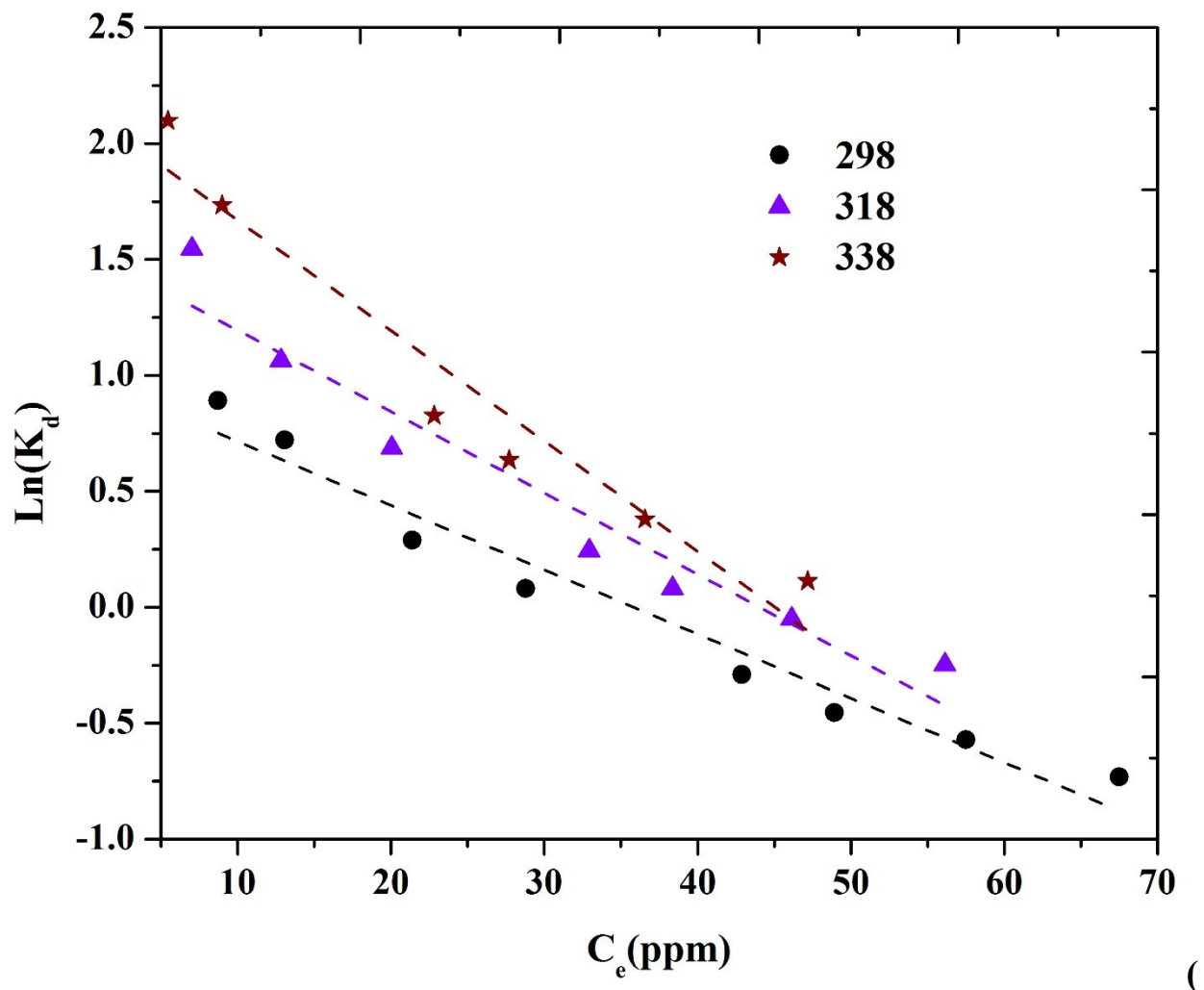
**Figure S10:** Transmission electron microscopy (TEM) images of (a) Fe<sub>3</sub>O<sub>4</sub> NPs bulk, and (b) Fe<sub>3</sub>O<sub>4</sub> NPs on the surface of graphene sheet.



(a)

Table S1: Constants of linear fit of  $\ln K_d$  Vs.  $C_e$  ( $\ln K_d = A + BC_e$ ) for  $\text{Co}^{2+}$  removal onto M-RGO.

T(K)	A	B	R <sup>2</sup>
298	1.7	-0.04	0.91
318	2.0	-0.044	0.95
338	2.4	-0.056	0.98



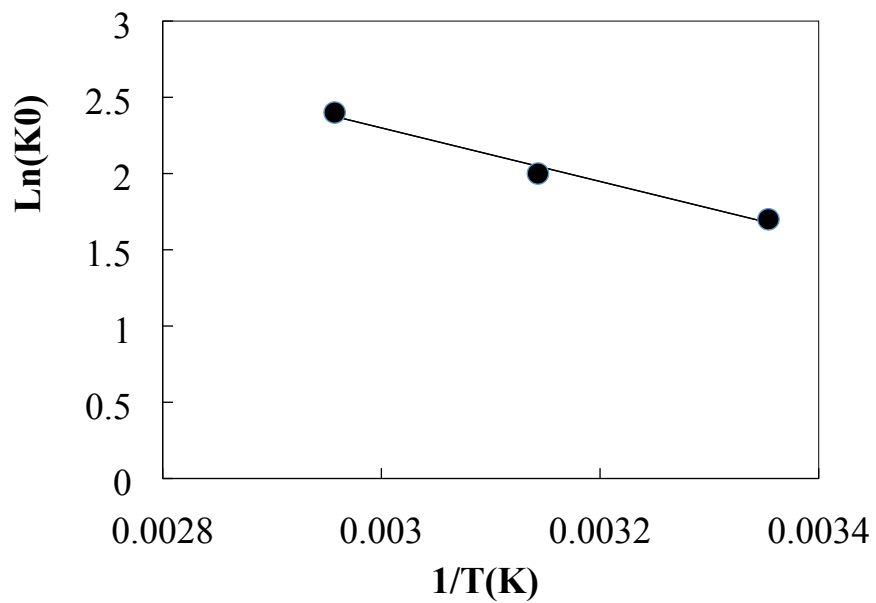
b)

Table S2: Constants of linear fit of  $\ln K_d$  Vs.  $C_e$  ( $\ln K_d = A + BC_e$ ) for  $\text{Sr}^{2+}$  removal onto M-RGO.

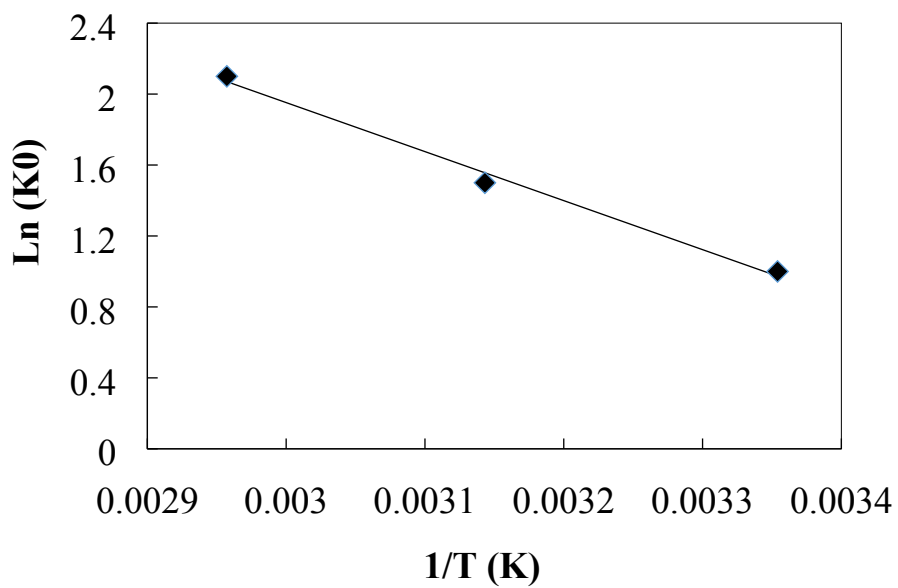
T(K)	A	B	R <sup>2</sup>
298	1.0	-0.027	0.96
318	1.5	-0.035	0.93
338	2.1	-0.047	0.93

Figure S11: Linear fitting of  $\ln K_d$  vs.  $C_e$  at pH=6.5 for (a)  $\text{Co}^{2+}$  ions; and (b)  $\text{Sr}^{2+}$  ions in aqueous solutions.





(a)



(b)

**Figure S12:** Vant't Hoff plot of  $\text{Ln}K^0$  versus  $1/T$  for (a)  $\text{Co}^{2+}$ , and (b)  $\text{Sr}^{2+}$  ions.

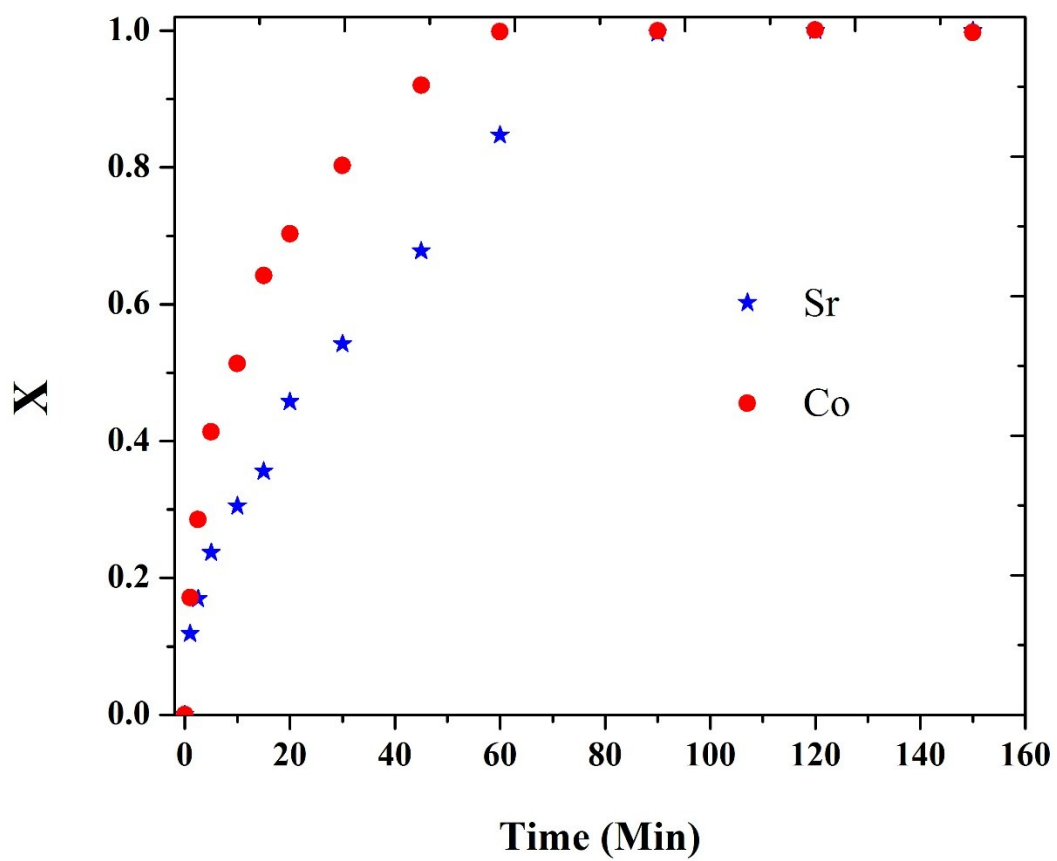


**Figure S13:** Comparison between the uptake rates in a normalized coordination (X).

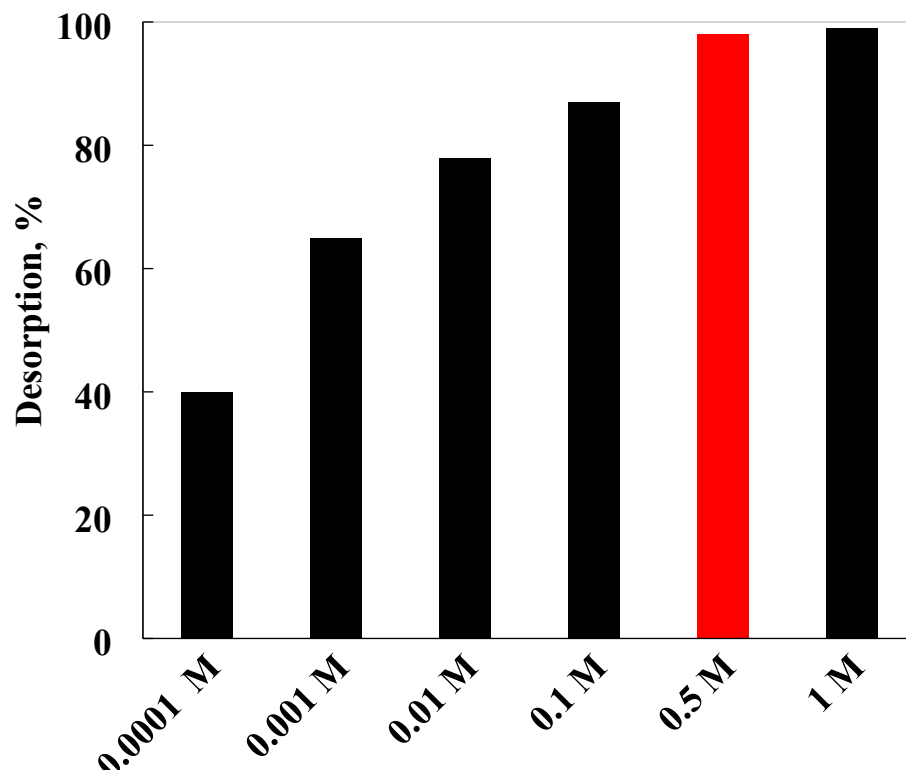


**Figure S14:** Desorption of Co<sup>2+</sup> ions from M-RGO using different concentration of hydrochloridric acid (HCl).